Bioresource Technology 196 (2015) 586–591

Contents lists available at ScienceDirect

Bioresource Technology

journal homepage: www.elsevier.com/locate/biortech

Structure and distribution of inorganic components in the cake layer of a membrane bioreactor treating municipal wastewater

Lijie Zhou [a,b], Siqing Xia [a,*], Lisa Alvarez-Cohen [b]

[a] State Key Laboratory of Pollution Control and Resource Reuse, College of Environmental Science and Engineering, Tongji University, 1239 Siping Road, Shanghai 200092, China
[b] Department of Civil and Environmental Engineering, University of California, Berkeley, CA 94720-1710, USA

HIGHLIGHTS

- Characterize the structure and distribution of the inorganic in cake layer of MBR.
- BCR, XPS and map/line scanning EDX identify the inorganic structure in cake layer.
- Si, Al, Ca, Mg, Fe, and Ba are the predominant inorganic compounds in cake layer.
- The predominant inorganic compounds are found to occur mostly as crystal particles.
- Si and Al accumulate together along the cross-sectional cake layer as SiO_2–Al_2O_3.

GRAPHICAL ABSTRACT

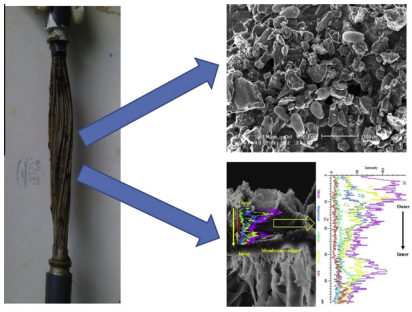

ARTICLE INFO

Article history:
Received 10 June 2015
Received in revised form 3 August 2015
Accepted 8 August 2015
Available online 14 August 2015

Keywords:
Membrane bioreactor
Cake layer
Inorganic distribution
BCR sequential extraction
SiO_2–Al_2O_3 crystal particles

ABSTRACT

A laboratory-scale submerged anoxic–oxic membrane bioreactor treating municipal wastewater was operated to investigate the structure and distribution of the inorganic cake layer buildup on the membrane. BCR (European Community Bureau of Reference) sequential extraction, X-ray photoelectron spectroscopy (XPS), and both map and line scan of energy-dispersive X-ray analysis (EDX) were performed for cake layer characterization. BCR results showed that Si, Al, Ca, Mg, Fe, and Ba were the predominant inorganic elements in the cake layer, and they occurred mostly as crystal particles. Crystal SiO_2 was the dominant inorganic compound while Ca in the form of $CaSO_4$ (dominant) and $CaCO_3$ were also present, but exerted little effect on the cake layer structure because most of these compounds were deposited as precipitates on the reactor bottom. EDX results indicated that Si and Al accumulated together along the cross-sectional cake layer in the form of Si–Al (SiO_2–Al_2O_3) crystal particles.

1. Introduction

Over the past decade, membrane bioreactors (MBRs) have been used increasingly often in municipal wastewater treatment as a means to increase effluent quality (Meng et al., 2007; Rui et al., 2005; Zhou et al., 2014a). However, membrane fouling can result in decreased membrane performance, reduced productivity and increased costs for cleaning and membrane replacement (Gao et al., 2011; Xia et al., 2008, 2012). Consequently, membrane fouling has become a key challenge for the application of MBRs. In recent studies, the accumulation of a sludge cake layer has been demonstrated to be the major contributor to membrane fouling in MBRs (Guo et al., 2012; Meng et al., 2009; Zhou et al., 2014c).

The deposition of sludge particles, colloids and solutes on the surface of a membrane generates a cake layer, with characteristics

* Corresponding author. Tel.: +86 21 65980440; fax: +86 21 65986313.
E-mail address: siqingxia@gmail.com (S. Xia).

http://dx.doi.org/10.1016/j.biortech.2015.08.026
0960-8524/

similar to porous media characterized by complex systems of connected inter-particle voids. The cake layer formation is a dynamic process, which can be classified into three general phases: (1) particulate cake initiation due to pore blocking; (2) cake formation due to deposition, accumulation and biological activity; and (3) cake compression (Zhang et al., 2006). Due to the dynamic formation process and the complex conditions within MBR systems, the structure of the cake layer is generally quite complicated. Overall, cake layers can be divided into organic (e.g. polysaccharides, peptidoglycan, proteins, cells and humic aggregates) and inorganic (e.g. colloids and inorganic precipitates such as silicates and calcium sulfate) components. In most studies, the organic components, especially soluble microbial products (SMP) and extracellular polymeric substances (EPS), have been considered the major contributors to cake layer formation and membrane fouling (Guo et al., 2012; Le-Clech et al., 2006; Meng et al., 2011).

The inorganic component of cake layers, which can also play a significant role in fouling, has been described in a variety of studies but has not yet been extensively characterized. For example, Kang et al. (2002) indicated that a thick cake layer composed of biomass and struvite formed on the membrane surface in a membrane-coupled anaerobic bioreactor while Lyko et al. (2007) found that inorganic compounds (mainly metal substances) were more important contributors to membrane fouling than biopolymers. Additionally, recent studies have focused on the fouling variations caused by specific inorganic components (such as Fe^{3+}, Ca^{2+}, Mg^{2+}, Cu^{2+}, CrO^{4-}, etc.), added as amendments in synthetic wastewater containing no insoluble compounds (Arabi and Nakhla, 2009; Katsou et al., 2011; Ognier et al., 2002; Zhang et al., 2008, 2006; Zhou et al., 2014b,c). In addition, Feng et al. (2013) studied fouling variation using municipal wastewater with specific heavy metal addition. Several papers demonstrated that the inorganic components within membrane cake layers are composed of elements such as Mg, Al, Fe, Ca, Si, etc. (Chen et al., 2012; Gao et al., 2011; Meng et al., 2011; Wang et al., 2008; Yang et al., 2011). However, these studies utilized spot-scan energy-dispersive X-ray analyzers (EDX) for cake component analysis, which is only capable of measuring the elemental distribution within a very small spot of the cake layer surface. No suitable method has yet been applied to characterize the detailed inorganic structure and distribution of inorganic components and their chemical structures in cake layers of MBRs treating municipal wastewater.

This study aims to develop an improved fundamental understanding of the structure and distribution of inorganic components in the fouling cake layers of MBR systems used for municipal wastewater treatment. A laboratory-scale submerged anoxic–oxic membrane bioreactor (A/O-MBR) was operated with municipal wastewater influent for over 90 days to characterize the cake layer by various methods. The BCR (European Community Bureau of Reference) sequential extraction, X-ray photoelectron spectroscopy (XPS), and both map scan and line scan of EDX were performed for characterization of the inorganic distribution along a cross-section of the cake layer.

2. Methods

2.1. A/O-MBR setup

For this study, a laboratory-scale A/O-MBR (Fig. 1) with a working volume of 4.5 L (anoxic and oxic zones of 1.5 L and 3.0 L, respectively) was operated for 90 days. A polyvinylidene fluoride hollow fiber membrane module (pore size 0.4 μm) with a total surface area of 260 cm^2 (Litree Company, China) was mounted in the oxic zone and a constant fluid flux was set at 17 L/($m^2 \cdot h$) with an intermittent suction mode (10 min suction and 2 min relaxation for each cycle). Air (0.4 m^3/h) was supplied continuously through a diffuser to provide oxygen for microbial activity and to induce a cross-flow action for effective scouring of the membrane surface. The air flow rate was adjusted with a gas flow-meter and transmembrane pressure (TMP) was monitored with a pressure gauge.

2.2. Operational condition

The effluent from an aerated grit chamber of the Quyang municipal wastewater treatment plant (WWTP) (Shanghai, China) treating municipal wastewater and storm water from residential areas and construction sites was used as influent to the anoxic MBR zone. Influent characteristics are shown in Table 1 and S1 (Supporting Information). The inoculating biomass was drawn from the return activated sludge stream in the Quyang WWTP. The newly inoculated A/O-MBR was initially operated for 60 days to achieve steady state for the acclimatization of activated sludge. The membrane module was then replaced with a new unit and the A/O-MBR was operated for 90 days for the experiments.

Hydraulic retention time (HRT) and solids retention time (SRT) were maintained at 10.0 h and 30 days, respectively. Mixed liquor suspended solids (MLSS) in the anoxic and oxic zones were approximately 3.8 ± 0.3 and 4.2 ± 0.5 g/L during the experiment, respectively. The flow rate of recycled mixed liquor from the oxic zone to the anoxic zone was controlled at 200% of the influent flow rate.

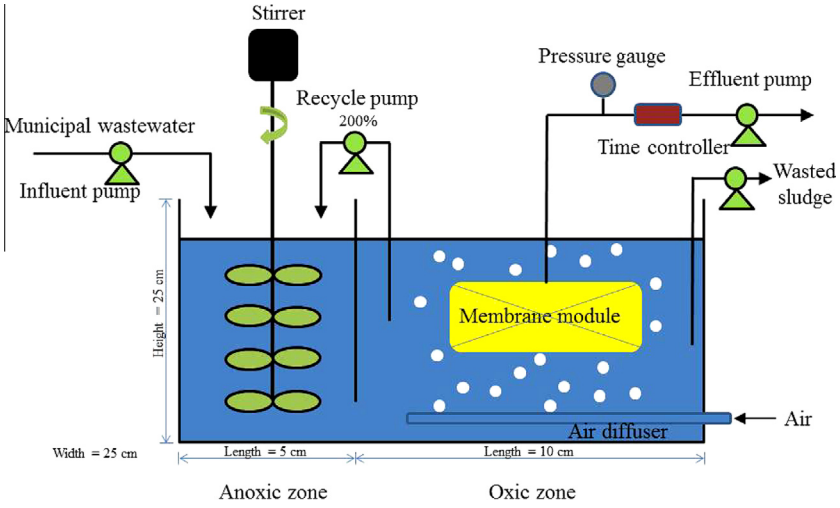

Fig. 1. A schematic of the anoxic/oxic membrane bioreactor used in this study.

Table 1
Inorganic compounds identified by the BCR sequential extraction procedure within each fraction of the membrane cake layer[a] and sludge (mg/dry sample g)[b] and average concentrations of inorganic compounds in the reactor influent and effluent (mg/L).[c]

	Zn	Ba	Fe	Mn	Mg	Ca	Cu	Al	Si
Cake layer									
F1	0.13 ± 0.02	0.02 ± 0.01	0.06 ± 0.01	0.27 ± 0.08	0.80 ± 0.08	4.4 ± 1.4	0.14 ± 0.03	0.05 ± 0.00	0.14 ± 0.04
F2	0.29 ± 0.04	0.00 ± 0.00	0.00 ± 0.00	0.00 ± 0.00	0.00 ± 0.00	0.00 ± 0.00	0.00 ± 0.01	0.00 ± 0.00	0.47 ± 0.09
F3	0.06 ± 0.01	0.05 ± 0.00	3.9 ± 1.3	0.03 ± 0.00	0.44 ± 0.09	0.60 ± 0.05	0.20 ± 0.03	1.9 ± 0.5	0.85 ± 0.31
F4	0.16 ± 0.01	5.6 ± 0.4	8.2 ± 1.5	0.08 ± 0.02	1.1 ± 0.1	9.8 ± 0.3	0.02 ± 0.00	26 ± 2	144 ± 13
Sludge									
F1	0.21 ± 0.05	0.02 ± 0.01	0.05 ± 0.00	0.54 ± 0.03	2.1 ± 0.5	7.1 ± 1.0	0.12 ± 0.01	0.06 ± 0.01	0.19 ± 0.03
F2	0.43 ± 0.11	0.17 ± 0.03	2.2 ± 0.1	0.61 ± 0.14	0.87 ± 0.45	5.0 ± 0.9	0.12 ± 0.03	0.88 ± 0.03	0.63 ± 0.11
F3	0.07 ± 0.01	0.07 ± 0.01	5.2 ± 1.1	0.04 ± 0.01	0.27 ± 0.08	0.52 ± 0.41	0.26 ± 0.08	1.9 ± 0.1	0.62 ± 0.18
F4	0.23 ± 0.10	0.07 ± 0.02	4.6 ± 1.0	0.04 ± 0.00	2.6 ± 0.3	8.5 ± 1.3	0.02 ± 0.00	11 ± 1	94 ± 2
Influent									
Total	1.2 ± 0.3	0.34 ± 0.24	6.1 ± 3.1	0.51 ± 0.41	13 ± 2	110 ± 4	0.29 ± 0.14	12 ± 13	360 ± 40
Soluble	0.08 ± 0.03	0.03 ± 0.02	0.46 ± 0.31	0.02 ± 0.01	8.1 ± 2.7	41 ± 6	0.04 ± 0.01	0.48 ± 0.13	31 ± 5
Effluent[d]	0.06 ± 0.02	0.11 ± 0.13	0.02 ± 0.00	0.00 ± 0.00	8.1 ± 1.5	40 ± 3	0.00 ± 0.00	0.01 ± 0.00	28 ± 5

[a] The BCR sequential extraction procedure within each fraction of the membrane cake layer was performed in triplicate when the operation of the membrane stopped (TMP = 40 kPa): $n = 12$.
[b] The BCR sequential extraction procedure within each fraction of sludge was performed in triplicate every 15 days: $n = 18$.
[c] Average concentrations of inorganic compounds in the reactor influent and effluent were measured every 3 days: $n = 30$.
[d] Due to the separation performed by the membrane, all reported elements in the effluent were in the soluble fraction.

The pH in the reactor was controlled by NaOH and HCl addition within the range of 7.0–7.7 and the reactor temperature was kept at 25–29 °C. When TMP reached 40 kPa, the membrane module was removed for physical (washing with tap water) or chemical cleaning (2% NaClO followed by 1% citric acid immersion, each for 4 h, per the manufacturer's instruction) prior to the next run.

2.3. Analytical methods

2.3.1. Membrane resistance analysis

It is common to interpret the overall resistance R as the sum of individual resistances (Guo et al., 2008). The hydraulic resistance can be calculated using the following equation:

$$R_t = R_m + R_p + R_c + R_i \quad (1)$$

$$R_n = \frac{\Delta P}{\mu J} \quad (2)$$

where R_m is the resistance of the clean membrane, R_p is the resistance due to concentration polarization, R_i is the pore blocking resistance and R_c is the fouling layer resistance. n is t, m, p, c or i, ΔP is TMP, J is permeate flux, μ is viscosity of the permeate water. The method to calculate the resistances of the membrane is as follows: (1) R_t – the flux and TMP of the membrane module were measured at the end of the operation period with activated sludge; (2) R_m – the flux and TMP of the new membrane module were measured before operation using deionized water; (3) R_p – the flux and TMP of the membrane at the end of the operation period were measured using deionized water and the result was subtracted from R_t to get R_p; (4) R_i – after physical cleaning was applied to remove the cake attached to the membrane, the flux and TMP were measured using deionized water and R_m was subtracted from the result to get R_i; (5) $R_c - R_m$, R_i and R_p were subtracted from R_t to get R_c.

2.3.2. Inorganic elements concentrations

The concentrations of inorganic elements in the influent, effluent, sludge and cake layer were analyzed via an inductively coupled plasma-optical emission spectrometer (ICP-OES, Optima 2100 DV, Perkin Elmer, USA) according to the Standard Methods (China-NEPA, 2002).

2.3.3. Analysis of XPS and XRD (X-ray diffraction)

The biopolymer sample was scraped from the cake layer of the fouled membrane modules and freeze-dried for 48 h prior to XPS (PHI-5000C ESCA, Perkin Elmer, USA) analysis and XRD (Bruker Optik GmbH, Ettlingen, Germany) analysis according to methods described in Jarde et al. (2005) and Salaita and Tate (1998). The XPS data was analyzed using the software of Auger Scan320Demo.

2.3.4. SEM-EDX (scanning electron microscopy-energy-dispersive X-ray analyzer) analysis

To characterize the cake layer, a piece of the membrane was cut from the middle part of the membrane module after freezing in liquid-nitrogen at the end of operation (when TMP = 40 kPa). 3 replicate samples and 8 spots in each sample were measured for the SEM-EDX analysis. Comparing pretreatments of the cake layer with glutaraldehyde and phosphate buffer to freezing with liquid-nitrogen, the liquid-nitrogen-freezing method better preserved the profile of the cake layer and resulted in minimal disturbance of the original metal distribution. The membrane cake layer was characterized with SEM (XL30, Philips, Netherlands) coupled with an EDX (Oxford Isis, UK).

2.3.5. BCR sequential extraction

Inorganic components in the cake layer and the sludge were differentiated into four fractions (the residuals were added as the fourth fraction) according to the BCR (the European Community Bureau of Reference) sequential extraction procedure (Peruzzi et al., 2011; Rauret et al., 1999):

(F1) *Exchangeable fraction associated with carbonates*. Metals are adsorbed on the sludge components and iron and manganese hydroxides. This is the most mobile fraction and is potentially toxic for microorganisms.
(F2) *Reducible fraction associated with Fe and Mn oxides*. These oxides strongly bind the heavy metals, but these compounds are thermodynamically unstable in anoxic and acidic conditions.
(F3) *Organic matter-bound oxidizable fraction*. Although metals in the F3 form are generally stable due to the recalcitrance of typical humic organic matter, they can become soluble if the organic matter is biodegraded.

(F4) *Residual fraction*. The residual fraction that is generally considered to be inert, containing metals that are not extractable by the applied methods.

The inorganic elements in all freeze-dried samples of the cake layer and mixed liquor were fractionated according to BCR sequential extraction as described previously (Li et al., 2013; Rauret et al., 1999). Generally, BCR sequential extraction was applied for heavy metal extraction. In addition to traditional heavy metals (such as Cu, Zn, etc.), Mg, Ca, Al and Si were extracted using BCR sequential extraction with extraction efficiencies of 96 ± 4%. The concentrations of inorganic elements in each fraction were determined by ICP-OES (Optima 2100 DV, Perkin Elmer, USA). Each experiment was conducted in triplicate and the results reported were the average values.

2.3.6. Additional analysis

Determination of chemical oxygen demand (COD), ammonia nitrogen (NH_4^+-N), total phosphorus (TP), total nitrogen (TN) and MLSS were conducted in accordance with Standard Methods (China-NEPA, 2002).

3. Results and discussion

3.1. A/O-MBR performance and fouling behavior

During the operation period (90 days), the A/O-MBR system exhibited steady-state performance for treating municipal wastewater. The influent and effluent COD concentrations were maintained at approximately 160 ± 80 and 8 ± 9 mg/L, respectively, with a COD removal efficiency of 95 ± 1% (Table S1). The removal efficiency of NH_4^+-N, TN and TP were 96 ± 1%, 65 ± 2% and 56 ± 6%, indicating that the A/O-MBR performed well during the experiment.

The development rate of TMP is an important index for evaluating membrane performance in A/O-MBRs, as it directly reflects the extent of membrane fouling. The TMP increased steadily with time during the four stages of the 90-day A/O-MBR operation (Fig. 2). The new and chemically-cleaned modules (stages 1 and 3) exhibited lower (7.5 kPa) initial pressures and lower TMP rate increases (1.0 kPa/d) than the physically-cleaned modules (stages 2 and 4) (around 22 kPa and 2.2 kPa/d, respectively). The intrinsic membrane resistance (R_m), concentration polarization resistance (R_p), pore blocking resistance (R_i) and cake layer resistance (R_c) contributed 20%, 38%, 9% and 33%, respectively, to the total resistance (Table 2). It has previously been reported that concentration polarization resistance is associated with cake layer formation (Meng et al., 2007), suggesting that the cake layer is the main factor resulting in membrane fouling, which is in agreement with the data from this study.

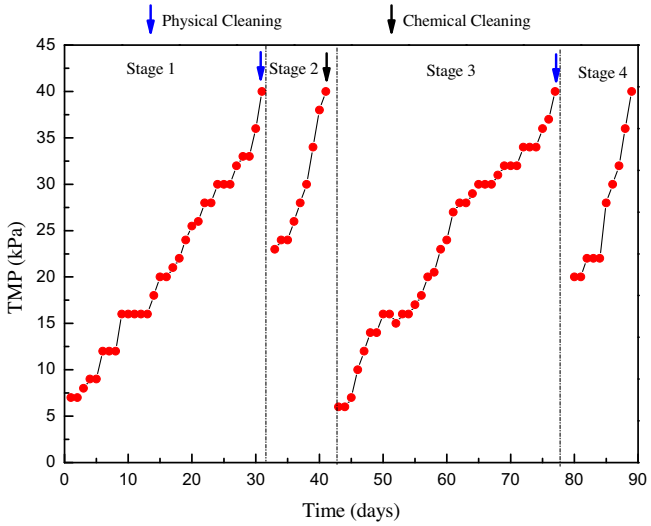

Fig. 2. Variations of TMP in A/O-MBR. The 4 stages of operation include stage 1 with a new membrane, stages 2 and 4 after physical membrane cleaning and stage 3 after chemical membrane cleaning. Physical cleaning only removes the cake layer while chemical cleaning removes both the cake layer and most materials, blocking the membrane pores.

3.2. Inorganic components and their structure in the cake layer

The inorganic components were classified into 4 fractions using the BCR sequential extraction procedure. The results for exchangeable (F1), reducible (F2), oxidizable (F3) and residual (F4) fractions of each inorganic element are presented in Table 1. The residual Si (144 mg/g) and residual Al (26 mg/g) were the major inorganic elements in the cake layer, which also contained Ba, Fe, Mg and Ca (trace Zn, Mn and Cu were also detected). The municipal wastewater in this study contained high concentrations of total (360 mg/L) and soluble Si (31 mg/L) (Table 1). Soluble Si in the influent was similar to that in the effluent (28 mg/L), indicating that most of the soluble Si flowed out with the effluent while insoluble Si was retained in the reactor. Other recent papers also reported that Si might be dominant in cake layers without characterizing the Si form (Guo et al., 2012; Meng et al., 2007; Yang et al., 2011). A comparison of Si in the cake layer and sludge indicates that the majority of the Si is retained in the cake layer with the dominant fraction residing in the residual insoluble fraction (F4). Consequently, in this study it is clear that the residual Si played a dominant role in the cake layer structure.

Ca and Mg have previously been identified as the major inorganic elements in membrane cake layers (Guo et al., 2012; Kang et al., 2002; Meng et al., 2005, 2009; Wang et al., 2008). However, in this study, the concentrations of Ca and Mg in the influent, cake layer and sludge were much lower than that of Si (Table 1), with Mg being especially low. It is interesting that Table 1 shows Ca concentrations of 110 mg/L in the influent and 40 mg/L in the effluent, with very little Ca in the sludge and cake layer. However, a significant amount of precipitate (Fig. S1) containing 130 mg Ca/g dry precipitate (Table S2) was found deposited at the bottom of reactor at the end of the treatment phase, particularly in the anoxic zone, representing significant sink for Ca within the reactor.

Fe and Al are commonly identified by SEM-EDX in cake layers of MBRs treating municipal wastewater (Meng et al., 2007; Yang et al., 2011). In this study, virtually all of the Fe and Al in the influent were retained in the A/O-MBR. Concentrations within the influent and effluent (Table 1) indicate that Fe and Al were significantly intercepted by the membrane and retained within the A/O-MBR system. Table 1 also shows that Al and Fe accumulated in the cake layer as part of the residual (F4) fraction. Moreover, the cake layer also contained a significant amount of residual Ba, even though influent Ba concentrations were low, indicating that Ba was effectively retained by the membrane.

XPS (Table 3 and Fig. S2) and XRD (Fig. S3) analyses were performed to further characterize the composition and structure of the inorganic cake layer components. Because of the low concentrations of most of the inorganic components in the cake layer and the sludge (Table 1), XPS analysis was only able to correctly identify the residual Al, Ca, Mg and Si (Table 3). Al and Si in both the cake layer and sludge were mainly in the form of Al_2O_3 and SiO_2 (XRD (Fig. S3) also predicted the crystal SiO_2–Al_2O_3 structures), respectively, indicating that residual SiO_2 was the major inorganic compound in the cake layer. Thus, inhibiting SiO_2 depo-

Table 2
Distribution of the membrane filtration resistance (R_t: total membrane resistance; R_m: intrinsic membrane resistance; R_p: concentration polarization resistance; R_c: cake layer resistance; R_i: pore blocking resistance)[a].

Resistance	R_t	R_m [b]	R_p	R_c	R_i
Value ($\times 10^{12}$ m^{-1})	2.70 ± 0.3	0.53 ± 0.05	1.00 ± 0.1	0.88 ± 0.07	0.25 ± 0.06
Percentage (%)	100	20 ± 3	38 ± 3	33 ± 2	9 ± 1

[a] The membrane filtration resistances (R_t, R_p, R_c and R_i) were measured in triplicate when the operation of the membrane stopped (TMP = 40 kPa): $n = 12$.
[b] In the stage 2 and 4, membrane only had the physical clean at the begin of operation. Therefore, R_m was analyzed in triplicate when the operation of the membrane stopped (TMP = 40 kPa) in the stage 1 and 3: $n = 6$. Additionally, R_m had little change at the initial operation according to the manufacture direction, which was similar as the fact of the long-term actual use in the lab.

Table 3
XPS analysis of inorganic compounds in the cake layer and sludge derived from the plots shown in Fig. S2.

	Al 2p		Ca 2p3		Mg 2p		Si 2p3	
	PBE[a] (A%)[b]	Comp.[c]	PBE[a] (A%)[b]	Comp.[c]	PBE[a] (A%)[b]	Comp.[c]	PBE[a] (A%)[b]	Comp.[c]
Cake layer	74.00 (94%)	Al_2O_3	346.40 (20%) 347.60 (74%)	$CaCO_3$ $CaSO_4$	51.60 (93%)	Mg(II)	102.60 (96%)	SiO_2
Sludge	74.00 (96%)	Al_2O_3	346.00 (31%) 347.20 (60%)	$CaCO_3$ $CaSO_4$	50.80 (66%) 52.80 (24%)	Mg(II)	101.80 (97%)	SiO_2

[a] PBE: peak binding energy.
[b] A%: area percentage.
[c] Comp.: suggested compound according to the XPS standard spectrum.

sition might be a promising method to control membrane fouling for this municipal wastewater. A number of previous studies characterizing membrane cake layer composition have postulated that residual Ca occurs as $CaCO_3$ and $CaSO_4$, with $CaCO_3$ as the dominant species (Demadis et al., 2005; Guo et al., 2012; Meng et al., 2009). However, data from this study (Fig. S2) shows that the peak area of $CaSO_4$ was over twice that of $CaCO_3$ in both the cake layer and the sludge, respectively, indicating that $CaSO_4$ was the dominant form here. Additionally, Fig. S1 and Table S2 demonstrate that $CaSO_4$ was the dominant form of Ca in the precipitate found at the bottom of the reactor. Because the pH within both the anoxic and oxic zones was controlled within the range of 7.0–7.7, carbonates and phosphates would be expected to be dominated by HCO_3^- and HPO_4^{2-}, respectively, inhibiting the precipitation of $CaCO_3$ and $Ca_3(PO_4)_2$. Due to the relatively high concentration of sulfate (14.5 mg/L) in the influent versus phosphate (2.1 mg/L) and the similar K_{sp} values ($K_{sp}(CaSO_4) = 3.16 \times 10^{-7}$; $K_{sp}(CaHPO_4) = 1.7 \times 10^{-7}$), $CaSO_4$ would be easier to precipitate than $CaHPO_4$ within the reactor. This explains why $CaSO_4$ was the dominant form of Ca and the occurrence of significant solids at the bottom of the anoxic zone, indicating that the MBR system effectively removed calcium by precipitation with SO_4^{2-} rather than with membrane interception. Finally, the XPS spectra of Mg unsurprisingly indicated that residual Mg in the cake layer was present in the form of Mg(II).

3.3. SEM-EDX analysis of the cake layer

To identify the distribution of inorganic materials in the membrane cake layer, SEM and both map scan and line scan EDX were performed in this study. The SEM image (250×) of the cake layer surface (Fig. S4) shows both areas with smooth surfaces (area A) and those with particle cover (area B), similar to results in other papers (Wang et al., 2008; Wei et al., 2011; Zhou et al., 2014b), Fig. S5 shows the inorganic distribution of the cake layer in 1000 × SEM images. C, O, Si and Al are distributed evenly throughout the smooth cake. Additionally, particles designated A and B in Fig. S5(a) mainly contain Si (dominant), O and Al, without other elements like C, Ca, Mg and Fe. Based on these results and those presented in Section 3.2, the particles were most likely made up of SiO_2 (dominant) and Al_2O_3 (minor).

Line scan EDX is a semiquantitative method to identify element distributions along a line to analyze the mass percent of elements. The cross-sectional distribution of the membrane cake layer (Fig. S6(a)) shows the thickness of the cake layer (~50 μm). The cross-sectional distribution of each inorganic element (Si, Al, Ca, Mg and Fe) in the cake layer (Fig. S6(b)) is heterogeneous, suggesting that the inorganic element distribution on the surface of the cake layer reported in previous studies (Gao et al., 2011; Meng et al., 2007), may not effectively represent the inner inorganic structure of the cake layer. Scanning from the membrane surface outwards, the percentages of Fe and Ca first increase, then drop and maintain a stable fraction along the remainder of the cross-section. The percentage of Mg increased at approximately 25 μm outwards from the membrane. Along the entire cross-section, Si is the dominant element in the cake layer, which is in accord with results of Section 3.2. Additionally, it is interesting that the distribution trends of Si and Al are similar, suggesting that Si and Al accumulate in the cake layer simultaneously. According to both XPS and XRD results (Figs. S2 and S3), Si and Al are present in the form of Si–Al crystal particles (SiO_2–Al_2O_3). The form of Si–Al crystal particles may be due to the crystal characteristics of SiO_2 which tends to exhibit tetrahedral coordination ($[SiO_4]$), with 4 oxygen atoms surrounding a central Si atom (Fig. S7(a)). All 4 oxygen atoms of $[SiO_4]$ tetrahedron are then shared with Si or other metals. Additionally, the Al ionic radius of Al_2O_3 (0.044 nm) is close to the Si ionic radius of SiO_2 (0.039 nm) (Chen, 2010). So, oxygen atoms, especially on the surface of $[SiO_4]$, strongly bond to Al atoms of Al_2O_3 (Fig. S7(b)). In addition, Al^{3+} easily replaces Si of $[SiO_4]$ to become $[AlO_4^{5-}]$ (Fig. S7(b)) (Chen, 2010). Consequently, results indicate that Si and Al were in the form of Si–Al crystal particles (SiO_2–Al_2O_3) along the cross-section of the cake layer. Moreover, pressure suction and cake compression can induce high cross-membrane pressures (Fig. S7(c)), causing variations of Si–O bond length and Si–O coordination (Hazen and Finger, 1982), allowing Al atoms to replace Si atoms or attach to O atoms with similar bond length or coordination (Chen, 2010), accelerating the formation of new Si–Al crystals in the cake layer. Therefore,

it is not surprising that Si–Al crystal particles are the major inorganic fouling components distributed within the cross-section of the MBR cake layer.

4. Conclusions

The structure and distribution of inorganic components in the cake layer of a submerged A/O-MBR treating municipal wastewater were reported. Novel insights into the predominant inorganic materials, especially alumina/silicate crystals, in the cake layer structure are described. BCR results show that residual inorganic elements (mainly Si and Al) are the dominant fraction in the cake layer and that Ca is present in the form of $CaSO_4$ (dominant) and $CaCO_3$, but has little effect on the cake layer structure. EDX results indicate that Si and Al accumulate together along the cross-sectional membrane cake layer in the form of Si–Al (SiO_2–Al_2O_3) crystal particles.

Acknowledgements

This work was supported by the National Science and Technology Pillar Program (2013BAD21B03), the Fundamental Research Funds for the Central Universities, China Scholarship Council and 111 Project.

Appendix A. Supplementary data

Supplementary data associated with this article can be found, in the online version, at http://dx.doi.org/10.1016/j.biortech.2015.08.026.

References

Arabi, S., Nakhla, G., 2009. Impact of cation concentrations on fouling in membrane bioreactors. J. Membr. Sci. 343 (1–2), 110–118.
Chen, J.Z., 2010. Modern Crystal Chemistry (first ed.). In: Q.S. Zhu (Ed.), Modern Chemical Foundation Series, vol. 20, Science Press, Beijing, pp. 202–204.
Chen, W., Zhu, N.W., Zheng, X.Y., Xu, M., He, Y.J., 2012. The characteristics of membrane fouling in the process of A(2)/(O-MBR) treating municipal wastewater. J. Food Agric. Environ. 10 (2), 925–928.
China-NEPA, 2002. Water and Wastewater Monitoring Methods, fourth ed., Chinese Environmental Science Publishing House: Beijing, China.
Demadis, K.D., Neofotistou, E., Mavredaki, E., Tsiknakis, M., Sarigiannidou, E.-M., Katarachia, S.D., 2005. Inorganic foulants in membrane systems: chemical control strategies and the contribution of "green chemistry". Desalination 179 (1), 281–295.
Feng, B., Fang, Z., Hou, J.C., Ma, X., Huang, Y.L., Huang, L.Q., 2013. Effects of heavy metal wastewater on the anoxic/aerobic-membrane bioreactor bioprocess and membrane fouling. Bioresour. Technol. 142, 32–38.
Gao, W.J., Lin, H.J., Leung, K.T., Schraft, H., Liao, B.Q., 2011. Structure of cake layer in a submerged anaerobic membrane bioreactor. J. Membr. Sci. 374 (1–2), 110–120.
Guo, J.F., Xia, S.Q., Wang, R.C., Zhao, J.F., 2008. Study on membrane fouling of submerged membrane bioreactor in treating bathing wastewater. J. Environ. Sci.-China 20 (10), 1158–1167.
Guo, W., Ngo, H.-H., Li, J., 2012. A mini-review on membrane fouling. Bioresour. Technol. 122, 27–34.
Hazen, R.M., Finger, L.W., 1982. Comparative Crystal Chemistry: Temperature, Pressure, Composition and the Variation of Crystal Structure. J. Wiley.
Jarde, E., Mansuy, L., Faure, P., 2005. Organic markers in the lipidic fraction of sewage sludges. Water Res. 39 (7), 1215–1232.
Kang, I.-J., Yoon, S.-H., Lee, C.-H., 2002. Comparison of the filtration characteristics of organic and inorganic membranes in a membrane-coupled anaerobic bioreactor. Water Res. 36 (7), 1803–1813.
Katsou, E., Malamis, S., Loizidou, M., 2011. Performance of a membrane bioreactor used for the treatment of wastewater contaminated with heavy metals. Bioresour. Technol. 102 (6), 4325–4332.
Le-Clech, P., Chen, V., Fane, T.A.G., 2006. Fouling in membrane bioreactors used in wastewater treatment. J. Membr. Sci. 284 (1–2), 17–53.
Li, H.M., Qian, X., Hu, W., Wang, Y.L., Gao, H.L., 2013. Chemical speciation and human health risk of trace metals in urban street dusts from a metropolitan city, Nanjing, SE China. Sci. Total Environ. 456, 212–221.
Lyko, S., Al-Halbouni, D., Wintgens, T., Janot, A., Hollender, J., Dott, W., Melin, T., 2007. Polymeric compounds in activated sludge supernatant—characterisation and retention mechanisms at a full-scale municipal membrane bioreactor. Water Res. 41 (17), 3894–3902.
Meng, F., Zhang, H., Li, Y., Zhang, X., Yang, F., Xiao, J., 2005. Cake layer morphology in microfiltration of activated sludge wastewater based on fractal analysis. Sep. Purif. Technol. 44 (3), 250–257.
Meng, F.G., Zhang, H.M., Yang, F.L., Liu, L.F., 2007. Characterization of cake layer in submerged membrane bioreactor. Environ. Sci. Technol. 41 (11), 4065–4070.
Meng, F.G., Chae, S.R., Drews, A., Kraume, M., Shin, H.S., Yang, F.L., 2009. Recent advances in membrane bioreactors (MBRs): membrane fouling and membrane material. Water Res. 43 (6), 1489–1512.
Meng, F.G., Zhou, Z.B., Ni, B.J., Zheng, X., Huang, G.C., Jia, X.S., Li, S.Y., Xiong, Y., Kraume, M., 2011. Characterization of the size-fractionated biomacromolecules: tracking their role and fate in a membrane bioreactor. Water Res. 45 (15), 4661–4671.
Ognier, S., Wisniewski, C., Grasmick, A., 2002. Characterisation and modelling of fouling in membrane bioreactors. Desalination 146 (1–3), 141–147.
Peruzzi, E., Masciandaro, G., Macci, C., Doni, S., Ravelo, S.G.M., Peruzzi, P., Ceccanti, B., 2011. Heavy metal fractionation and organic matter stabilization in sewage sludge treatment wetlands. Ecol. Eng. 37 (5), 771–778.
Rauret, G., Lopez-Sanchez, J., Sahuquillo, A., Rubio, R., Davidson, C., Ure, A., Quevauviller, P., 1999. Improvement of the BCR three step sequential extraction procedure prior to the certification of new sediment and soil reference materials. J. Environ. Monit. 1 (1), 57–61.
Rui, L., Xia, H., Chen, L.J., Wen, X.H., Yi, Q., 2005. Operational performance of a submerged membrane bioreactor for reclamation of bath wastewater. Process Biochem. 40 (1), 125–130.
Salaita, G.N., Tate, P.H., 1998. Spectroscopic and microscopic characterization of Portland cement based unleached and leached solidified waste. Appl. Surf. Sci. 133 (1–2), 33–46.
Wang, Z.W., Wu, Z.C., Yin, X., Tian, L.M., 2008. Membrane fouling in a submerged membrane bioreactor (MBR) under sub-critical flux operation: membrane foulant and gel layer characterization. J. Membr. Sci. 325 (1), 238–244.
Wei, C.H., Huang, X., Ben Aim, R., Yamamoto, K., Amy, G., 2011. Critical flux and chemical cleaning-in-place during the long-term operation of a pilot-scale submerged membrane bioreactor for municipal wastewater treatment. Water Res. 45 (2), 863–871.
Xia, S.Q., Guo, J.F., Wang, R.C., 2008. Performance of a pilot-scale submerged membrane bioreactor (MBR) in treating bathing wastewater. Bioresour. Technol. 99 (15), 6834–6843.
Xia, S.Q., Jia, R.Y., Feng, F., Xie, K., Li, H.X., Jing, D.F., Xu, X.T., 2012. Effect of solids retention time on antibiotics removal performance and microbial communities in an A/O-MBR process. Bioresour. Technol. 106, 36–43.
Yang, X.L., Song, H.L., Chen, M., Cheng, B., 2011. Characterizing membrane foulants in MBR with addition of polyferric chloride to enhance phosphorus removal. Bioresour. Technol. 102 (20), 9490–9496.
Zhang, J., Chua, H.C., Zhou, J., Fane, A., 2006. Factors affecting the membrane performance in submerged membrane bioreactors. J. Membr. Sci. 284 (1), 54–66.
Zhang, H.F., Sun, B.S., Zhao, X.H., Gao, Z.H., 2008. Effect of ferric chloride on fouling in membrane bioreactor. Sep. Purif. Technol. 63 (2), 341–347.
Zhou, L., Zhang, Z., Jiang, W., Guo, W., Ngo, H.-H., Meng, X., Fan, J., Zhao, J., Xia, S., 2014a. Effects of low-concentration Cr(VI) on the performance and the membrane fouling of a submerged membrane bioreactor in the treatment of municipal wastewater. Biofouling 30 (1), 105–114.
Zhou, L., Zhang, Z., Meng, X., Fan, J., Xia, S., 2014b. New insight into the effects of Ca (II) on cake layer structure in submerged membrane bioreactors. Biofouling 30 (5), 571–578.
Zhou, L., Zhang, Z., Xia, S., Jiang, W., Ye, B., Xu, X., Gu, Z., Guo, W., Ngo, H.-H., Meng, X., Fan, J., Zhao, J., 2014c. Effects of suspended titanium dioxide nanoparticles on cake layer formation in submerged membrane bioreactor. Bioresour. Technol. 152, 101–106.